

Similar differences have been observed with isomers of Pt-(CH₃)₂Br(gly)₂⁻¹⁴

Discussion

Many platinum(IV) halo complexes are photolabilized.²³ The proposed mechanisms involve direct heterolysis of a platinum-(IV)-ligand bond. The reaction occurs from the lowest energy ligand field triplet excited state, which is reached by radiationless processes from the various ligand to metal charge-transfer excited states. This triplet state must involve electronic population of an "e_g" type orbital having antibonding character with respect to the metal-ligand σ bond.²³ We have no evidence for the mechanism of the reaction in our complexes, but in the discussion that follows, we will assume that it also proceeds through a triplet excited state. Since our complexes have much lower symmetry than octahedral, the two "e_g" type orbitals, which we shall label (d_{z²})^{*} and (d_{x²-y²})^{*} will differ in energy. Furthermore, since methyl ligands have a high ligand field²⁴ and lie in the *xy* plane of the molecule, the (d_{x²-y²})^{*} orbital will be higher in energy than (d_{z²})^{*}. The lowest energy triplet state would therefore be expected to be that in which the (d_{z²})^{*} orbital is populated. Occupancy of this antibonding orbital would weaken all the platinum-ligand bonds, but especially those along the *z* (Br-Pt-O) axis. Weakening or breaking of the Pt-O bond in **9** allows migration of nitrogen to this coordination site. This reaction is unusual among photochemical reactions of

Pt(IV) complexes, in that it is intramolecular. Side reactions at high pH, in which hydroxide replaces bromide, occur because the Pt-Br bond is also weakened. The reverse reaction, in which bromide reacts with Pt(CH₃)₂(OH)(mida)⁻ (**6a**), occurs only to a small extent on prolonged irradiation.

If the rule applies that the most stable isomer thermodynamically is the one in which ligands with the strongest trans influence are trans to ligands with the weakest trans influence,²⁵ then isomer **11**, in which the two weakest ligands (carboxyl) are trans to the two strongest (methyl), will be more stable than **9**, with one N atom trans to methyl. This would explain why the conversion of **9** into **11** is irreversible.

The photoisomerization reactions of dimethylbromoplatinum-(IV) complexes are of considerable synthetic utility. Combined with the kinetic effect provided by the high trans effect of the methyl ligands, they give us a fine control over the geometry of complexes with a wide variety of ligands. Mechanisms of the photochemical reactions are currently under investigation.

Acknowledgment. We thank the Australian Research Council for financial support. J.A.S., is grateful for the award of an Australian Postgraduate Research Award. We thank Dr. R. V. Tasker for carrying out some of the early experimental work.

Supplementary Material Available: Table SI, listing microanalytical data, and Tables SII and SIII, listing full NMR data (4 pages). Ordering information is given on any current masthead page.

(23) Ford, P. C.; Peterson, J. D.; Hintze, R. E. *Coord. Chem. Rev.* **1974**, *14*, 67.

(24) Chatt, J.; Hayter, R. G. *J. Chem. Soc.* **1961**, 772.

(25) Appleton, T. G.; Clark, H. C.; Manzer, L. E. *J. Organomet. Chem.* **1974**, *65*, 275.

Contribution from the Department of Chemistry, University of California at San Diego, La Jolla, California 92093

Pentacoordinate Zinc: Synthesis and Structures of Bis[1-(methylthio)-*cis*-stilbene-2-thiolato]zinc and of Its Adducts with Mono- and Bidentate Nitrogen Bases

Cheng Zhang, R. Chadha, H. K. Reddy, and G. N. Schrauzer*

Received October 2, 1990

1-(Methylthio)-*cis*-stilbene-2-thiol, Ph(SCH₃)C=C(SH)Ph, forms a dimeric μ -S-bridged zinc complex of composition Zn₂-[(CH₃)₂S₂C₂Ph₂]₄, containing equivalent pentacoordinate Zn(II) ions in a trigonal-bipyramidal ligand environment; Zn-S bond lengths vary from 2.270 (3) to 2.712 (3) Å (2.46 Å average), as determined by single-crystal X-ray analysis. It reacts with 4-(dimethylamino)pyridine to yield a monomeric adduct in which Zn(II) is also pentacoordinate and the coordination geometry is distorted square-pyramidal with Zn-N and average Zn-S bond lengths of 2.069 (10) and 2.48 (25) Å. In the 2,2'-bipyridine (bpy) adduct, the zinc atom is pentacoordinate as well, although one coordinate Zn-S(CH₃) bond is weak. The bpy ligand is symmetrically coordinated to zinc, with mean Zn-N bond distances of 2.097 (10) Å. One sulfur ligand is asymmetrically bidentate with one normal Zn-S bond of 2.292 (3) Å; the coordinative Zn-S(CH₃) bond of 3.124 (3) Å is long but still shorter than the sum of the van der Waals radii. The other sulfur ligand is monodentate, the Zn-S bond length is 2.275 (3) Å, and the -S-CH₃ group is in a noninteractive position. The nitrogen ligands exchange with free ligands in solution, as evidenced by variable-temperature ¹H NMR measurements. The preferred adoption by Zn(II) of pentacoordinated structures under conditions where tetra- and hexacoordination are possible with identical probabilities suggests that pentacoordination is energetically favored and may be important in biological systems.

Complexes of zinc with S₄, S₃N, or S₂N₂ ligand cores are of interest as structural models of the immediate ligand environment of zinc in DNA-binding proteins and certain zinc-containing enzymes. While zinc is usually assumed to be tetra-coordinate and this is probably true for the resting state of the biological systems, this need not necessarily be the case for their functional states, where the possibility exists that zinc adopts penta-, tri-, and perhaps even hexacoordinated structures. For example, a reactive intermediate with pentacoordinated zinc has been proposed in the reversible hydration of CO₂ by carbonic anhydrase¹

and in liver alcohol dehydrogenase.² Pentacoordinated complexes of zinc are known but are relatively rare. A 1983 survey³ listed 33 structurally characterized examples among 379 mostly tetra-coordinated entries. Tricoordination is probably favored in anionic complexes, as evidenced by the recent⁴ characterization of the trigonal-planar anion Zn(SR)₃⁻, where R = 2,3,5,6-Me₄C₆H, while hexacoordinated structures could be expected to occur preferentially in cationic complexes; one example is the recently reported Zn(II) complex of 1,4,7-trithiacyclononane.⁵

(1) (a) Gupta, R. K.; Pesando, J. M. *J. Biol. Chem.* **1975**, *250*, 2630. (b) Kannan, K. K.; Pelef, M.; Fridborg, K.; Cid-Dresner, M.; Lougren, S. *FEBS Lett.* **1977**, *73*, 115.

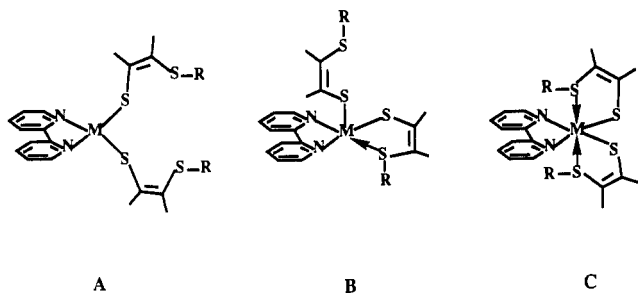
(2) Dworschach, R. T.; Plapp, B. V. *Biochemistry* **1977**, *16*, 2716.

(3) Auf der Heyde, T. P. E.; Nassimbeni, L. R. *Acta Crystallogr.* **1984**, *B40*, 582.

(4) Gruff, E. S.; Koch, S. A. *J. Am. Chem. Soc.* **1989**, *111*, 8762.

As most of the zinc complexes with unusual coordination numbers were discovered more by accident than by design, or with special ligand systems, the origin of pentacoordination is still essentially unknown.

Our ongoing studies of complexes of unsaturated sulfur ligands, notably of 1-(methylthio)-*cis*-stilbene-2-thiol, $\text{Ph}(\text{SCH}_3)\text{C}=\text{C}(\text{SH})\text{Ph}$ (**1**), have established that these are facultative monodentate, bidentate, and μ -S bridging ligands which may be used as molecular probes of residual ligand affinities of metal ions in complexes. As an example of one such application, we herein report the synthesis and structures of zinc bis[1-(methylthio)-*cis*-stilbene-2-thiolate] (**2**) and of its adducts with 4-(dimethylamino)pyridine, *dmapy* (**3**), pyridine, *py* (**4**), and 2,2'-bipyridyl, *bpy* (**5**). In complexes **2**–**5**, zinc could in principle adopt tri-, tetra-, penta-, and even hexacoordinated structures depending on whether the ligands are coordinated in the monodentate, bidentate, or μ -S bridged fashion. The *bpy* adduct, **5**, is of particular interest in this context, as it could adopt tetra-, penta-, and hexacoordinated structures as shown in diagrams A–C.



On the basis of X-ray crystallographic structure determinations, we will demonstrate that Zn(II) in complexes **2**–**5** has a clear preference for pentacoordination in the solid state. In addition, the structures of the complexes in solution and their ligand-exchange reactions as measured by variable-temperature ^1H NMR spectroscopy will be discussed.

Experimental Section

All commercially available reagents and chemicals were of analytical or reagent grade purity and were used as received. The free thiol ligand, 1-(methylthio)-*cis*-stilbene-2-thiol, was prepared as described in ref 6. The ^1H NMR spectra were obtained on a GE QE-300 instrument at 300 MHz and on an EM-390 instrument at 90 MHz. Variable-temperature ^1H NMR studies were performed on the GE QE-300 instrument at 300 MHz monitored by the liquid-nitrogen-cooled probe. UV-vis spectra were recorded on a Beckman DU-40 spectrophotometer.

Synthesis of $\text{Zn}_2[\text{Ph}(\text{SCH}_3)\text{C}=\text{C}(\text{S})\text{Ph}]_4$ (2**).** Zinc chloride, 0.20 g (1.47 mmol), was dissolved in 20 mL of deionized water to form a clear solution, which was added, drop by drop, to 20 mL of an ethanol solution of 0.80 g (3.1 mmol) of **1**. To the resulting cloudy suspension was slowly added drop by drop a 1 N solution of NaOCH_3 in CH_3OH until the appearance of a white precipitate. The supernatant was decanted after 30 min, and the product was collected by filtration. After consecutive washing with 3×10 mL each of ethanol and *n*-hexane, the white solid was dried under vacuum, yielding 0.72 g (0.62 mmol) of **2**, mp 221 °C dec, corresponding to a yield of 84.4% based in ZnCl_2 . Anal. Calcd for $\text{C}_{60}\text{H}_{52}\text{S}_8\text{Zn}_2$: C, 62.11; H, 4.52; Zn, 11.27. Found: C, 62.35; H, 4.57; Zn, 11.03. ^1H NMR (25 °C, CD_2Cl_2): δ 7.17–7.10 (m, 40 H, Ph H), 2.35 (s, 12 H, $-\text{SCH}_3$).

Synthesis of $\text{Zn}[\text{Ph}(\text{SCH}_3)\text{C}=\text{C}(\text{S})\text{Ph}]_2(\text{dmapy})$ (3**), $\text{Zn}[\text{Ph}(\text{SCH}_3)\text{C}=\text{C}(\text{S})\text{Ph}]_2(\text{py})$ (**4**), and $\text{Zn}[\text{Ph}(\text{SCH}_3)\text{C}=\text{C}(\text{S})\text{Ph}]_2(\text{bpy})$ (**5**).** Complex **2**, 0.20 g (0.17 mmol), was placed into a Schlenk tube of 150-mL capacity and suspended in 10 mL of CH_2Cl_2 . To this suspension was added 0.10 g (0.86 mmol) of *dmapy* to form a clear solution after stirring for several minutes; this was followed by the addition of 10 mL of *n*-hexane. The colorless precipitate that formed overnight was collected and washed with *n*-hexane, affording 0.23 g of **3** (0.33 mmol), corresponding to 96% yield based on **2**; mp 110 °C dec. Anal. Calcd for $\text{C}_{37}\text{H}_{36}\text{N}_2\text{S}_4\text{Zn}$: C, 63.28; H, 5.17; N, 3.99. Found: C, 63.08; H, 5.25;

Table I. Crystallographic Data Collection Parameters for **2**, **3**, and **5**

	2	3	5
formula	$\text{C}_{60}\text{H}_{52}\text{S}_8\text{Zn}_2$	$\text{C}_{37}\text{H}_{37}\text{N}_2\text{S}_4\text{Zn}$	$\text{C}_{40.5}\text{H}_{35}\text{N}_2\text{S}_4\text{ClZn}$
space group	$P\bar{1}$	$P1$	$P2_1/c$
<i>a</i> , Å	8.5025 (14)	9.0887 (16)	13.850 (3)
<i>b</i> , Å	16.070 (5)	9.674 (2)	17.611 (3)
<i>c</i> , Å	21.683 (7)	11.377 (2)	16.626 (4)
α , deg	90	81.740 (16)	
β , deg	90	74.769 (15)	98.47 (2)
γ , deg	90	62.962 (14)	
<i>V</i> , Å ³	2787.9 (13)	859.4 (3)	4011.3 (15)
<i>Z</i>	2	1	4
fw	1160.2	703.3	778.8
d_{calcd} , g/cm ³	1.382	1.359 ^a	1.290
μ , cm ⁻¹	1.206	0.992	0.922
$\lambda(\text{Mo K}\alpha)$, Å	0.71073	0.71073	0.71073
<i>T</i> , K	297	297	297
<i>R</i> (F_o)	0.0522	0.0604	0.0601
<i>R</i> _w (F_o)	0.0491	0.0604	0.0826

$$^a d_{\text{meas}} = 1.36 \text{ g/cm}^3.$$

N, 3.87. ^1H NMR (25 °C, CDCl_3): δ 8.50 (d, $J = 6.3$ Hz, 2 H, *dmapy* H (2, 6)), 7.26–6.95 (m, 20 H, Ph H), 6.61 (d, $J = 6.3$ Hz, 2 H, *dmapy* H (3, 5)), 3.91 (s, 6 H, $-\text{NCH}_3$), 1.97 (s, 6 H, $-\text{SCH}_3$).

The 1:1 pyridine adduct **4** was obtained analogously from 0.20 g (0.17 mmol) of **2** and 0.10 mL (1.26 mmol) of *py*, in the form of colorless crystals: mp 65 °C dec; yield 0.22 g (90% based on **2**). Anal. Calcd for $\text{C}_{35}\text{H}_{31}\text{NS}_4\text{Zn}$: C, 63.77; H, 4.74; N, 2.12. Found: C, 64.01; H, 4.77; N, 2.14. ^1H NMR (25 °C, CDCl_3): δ 8.89 (d, $J = 6.0$ Hz, 2 H, *py* H (2, 6)), 7.87 (t, $J = 7.5$ Hz, 1 H, *py* H (4)), 7.49 (t, $J = 6.9$ Hz, 2 H, *py* H (3, 5)), 7.25–7.02 (m, 20 H, Ph H), 2.11 (s, 6 H, $-\text{SCH}_3$).

The *bpy* adduct **5** was obtained analogously from 0.20 g (0.17 mmol) of **2** and 0.11 mg (0.74 mmol) of *bpy*, in the form of orange crystals: mp 110 °C dec; yield 0.22 g (0.30 mmol), 88% based on **2**. Anal. Calcd for $\text{C}_{40}\text{H}_{34}\text{N}_2\text{S}_4\text{Zn}$: C, 65.25; H, 4.65; N, 3.80. Found: C, 65.52; H, 4.78; N, 3.91. ^1H NMR (25 °C, CDCl_3): δ 8.65 (d, $J = 4.8$ Hz, 2 H, *bpy* H (2, 9)), 8.06 (d, $J = 8.1$ Hz, 2 H, *bpy* H (5, 6)), 7.88 (t, $J = 7.2$ Hz, 2 H, *bpy* H (3, 8)), 7.40 (t, $J = 6.3$ Hz, 2 H, *bpy* H (4, 7)), 7.06–6.78 (m, 20 H, Ph H), 2.09 (s, 6 H, $-\text{SCH}_3$).

Variable-Temperature NMR Study. 5:bpy = 1:0.85. The data are represented by Figure 4, and they are given in the supplementary material.

5:dmapy = 1:0.5. ^1H NMR (–90 °C, CD_2Cl_2): δ 8.63 (d, $J = 4.2$ Hz, Zn–*bpy* H (2, 9)), 8.57 (d, $J = 4.8$ Hz, *bpy* H (2, 9)), 8.38 (d, $J = 7.5$ Hz, Zn–*dmapy* and *dmapy* H (2, 6)), 7.93 (t, $J = 7.8$ Hz, *bpy* H (5, 6)), 7.84 (t, $J = 8.1$ Hz, Zn–*bpy* H (5, 6) and Zn–*bpy* H (3, 8)), 7.55 (t, $J = 6.0$ Hz, *bpy* H (4, 7)), 7.34 (t, $J = 6.3$ Hz, Zn–*bpy* H (4, 7)), 6.62 (d, Zn–*dmapy* and *dmapy* H (3, 5)), 3.02 (s, Zn–*dmapy* H), 2.97 (s, *dmapy* H), 1.83 (s, (*bpy*)Zn– SCH_3), 1.61 (s, (*dmapy*)Zn– SCH_3). ^1H NMR (20 °C, CD_2Cl_2): δ 8.65 (d, $J = 4.8$ Hz, Zn–*bpy* and *bpy* H (2, 9)), 8.46 (d, $J = 6.6$ Hz, Zn–*dmapy* and *dmapy* H (2, 6)), 8.17 (d, $J = 4.2$ Hz, Zn–*bpy* and *bpy* H (5, 6)), 7.91 (t, $J = 7.5$ Hz, Zn–*bpy* and *bpy* H (3, 8)), 7.43 (t, $J = 6.0$ Hz, Zn–*bpy* and *bpy* H (4, 7)), 6.96 (m, Ph H), 6.67 (d, $J = 6.6$ Hz, Zn–*dmapy* and *dmapy* H).

2 in Moist Solvent. ^1H NMR (0 °C, CD_2Cl_2): δ 7.14–7.07 (m, 40 H, Ph H), 2.25 (s, 12 H, $-\text{SCH}_3$). ^1H NMR (–60 °C, CD_2Cl_2): δ 7.34–6.98 (m, 40 H, Ph H), 2.24 (s, Zn dimer $-\text{SCH}_3$), 1.96 (s, HOH), 1.19 (s, Zn hydrate $-\text{SCH}_3$). [UV-vis ($n-\pi^*$ transition only): $\lambda_{\text{max}} = 450$ nm ($\epsilon = 600$)]

Thermolysis Studies. Complex **2**, 0.2 g, was heated to 250 °C in a small vacuum sublimation apparatus to yield 0.1 g of a pale yellow sublimate, mp 90 °C, identified as *cis*-bis(methylthio)stilbene by comparison of its ^1H NMR spectra in CDCl_3 with that of an authentic sample. The pale red-brown nonvolatile residue was identified as $[\text{Zn}(\text{S}_2\text{C}_2\text{Ph}_2)]_x$ (**6**), mp 300 °C dec. Anal. Calcd for $\text{C}_{14}\text{H}_{10}\text{S}_2\text{Zn}$: C, 54.64; H, 3.28; S, 20.84. Found: C, 54.94; H, 3.31; S, 21.05.

X-ray Structure Analyses of Complexes 2, 3, and 5. Crystals of complexes **2** and **3** sealed into capillaries and a crystal of **5** fixed on a glass fiber were mounted on a Nicolet R3m/V diffractometer for X-ray data collection; crystal dimensions and other relevant data are summarized in Table I. The positions of the Zn and S atoms were obtained from the automatic direct-methods routine of the program SHELXTL-PLUS, the positions of remaining non-hydrogen atoms were determined from a difference Fourier map. All atoms were refined anisotropically. Hydrogen atoms were included in ideal positions with *U* fixed at 0.08 Å². Refinements gave the final values of *R* and *R*_w listed in Table I. The final difference map of each compound had no feature of any chemical significance, though a few residual peaks were apparent whose density did

(5) Kueppers, H. J.; Wieghardt, K.; Nuber, B.; Weiss, J. *Z. Anorg. Allg. Chem.* **1989**, *577*, 155.

(6) Schrauzer, G. N.; Zhang, C.; Schlemper, E. O. *Inorg. Chem.* **1990**, *29*, 3371.

Table II. Selected Geometrical Data for 2

Distances (Å)			
Zn(1)-S(1)	2.450 (3)	Zn(1)-S(2)	2.712 (3)
Zn(1)-S(3)	2.270 (3)	Zn(1)-S(4)	2.548 (3)
Zn(1a)-S(1)	2.383 (3)	S(2)-C(2)	1.802 (10)
S(1)-C(10a)	1.787 (10)	S(3)-C(30)	1.758 (9)
S(2)-C(20)	1.761 (11)	S(4)-C(40)	1.770 (9)
S(4)-C(4)	1.806 (10)		

Angles (deg)			
Zn(1)-S(1)-Zn(1a)	84.2 (1)	Zn(1)-S(1)-C(10a)	105.8 (3)
Zn(1a)-S(1)-C(10a)	107.4 (3)	Zn(1)-S(2)-C(2)	112.0 (4)
Zn(1)-S(2)-C(20)	100.1 (3)	C(2)-S(2)-C(20)	104.4 (5)
Zn(1)-S(3)-C(30)	103.7 (3)	Zn(1)-S(4)-C(4)	107.9 (4)
Zn(1)-S(4)-C(40)	99.7 (3)	C(4)-S(4)-C(40)	102.9 (4)
C(20)-C(10)-C(11)	122.7 (9)	C(20)-C(10)-S(1a)	124.4 (8)
C(11)-C(10)-S(1a)	112.7 (7)	S(2)-C(20)-C(10)	121.5 (8)
S(2)-C(20)-C(21)	116.9 (7)	C(10)-C(20)-C(21)	121.1 (9)
S(3)-C(30)-C(40)	128.3 (7)	S(3)-C(30)-C(31)	111.9 (7)
C(40)-C(30)-C(31)	119.8 (8)	S(4)-C(40)-C(30)	120.5 (6)
S(4)-C(40)-C(41)	115.4 (7)	C(30)-C(40)-C(41)	124.1 (8)
S(1)-Zn(1)-S(2)	87.5 (1)	S(1)-Zn(1)-S(3)	123.5 (1)
S(2)-Zn(1)-S(3)	92.2 (1)	S(1)-Zn(1)-S(4)	99.3 (1)
S(2)-Zn(1)-S(4)	172.0 (1)	S(3)-Zn(1)-S(4)	87.5 (1)
S(1)-Zn(1)-S(1a)	95.8 (1)	S(2)-Zn(1)-S(1a)	80.1 (1)
S(3)-Zn(1)-S(1a)	139.7 (1)	S(4)-Zn(1)-S(1a)	95.0 (1)

Table III. Selected Geometrical Data for 3

Distances (Å)			
Zn(1)-S(1)	2.219 (8)	Zn(1)-S(2)	2.513 (7)
Zn(1)-S(3)	2.831 (7)	Zn(1)-S(4)	2.378 (9)
Zn(1)-N(1)	2.069 (10)	S(2)-C(8)	1.659 (23)
S(1)-C(10)	1.733 (19)	S(3)-C(9)	1.969 (25)
S(2)-C(20)	1.727 (15)	S(4)-C(40)	1.768 (16)
S(3)-C(30)	1.848 (24)		

Angles (deg)			
S(1)-Zn(1)-S(2)	86.3 (3)	S(2)-Zn(1)-S(3)	153.1 (2)
S(1)-Zn(1)-S(3)	88.8 (2)	S(1)-Zn(1)-S(4)	146.3 (2)
S(2)-Zn(1)-S(4)	93.7 (3)	S(3)-Zn(1)-S(4)	76.1 (2)
S(2)-Zn(1)-N(1)	108.5 (3)	S(1)-Zn(1)-N(1)	107.5 (4)
S(4)-Zn(1)-N(1)	104.4 (4)	S(3)-Zn(1)-N(1)	98.2 (3)
Zn(1)-S(1)-C(10)	106.1 (9)	Zn(1)-S(2)-C(20)	101.0 (5)
Zn(1)-S(2)-C(8)	117.8 (7)	Zn(1)-S(3)-Zn(2)	28.8 (1)
C(8)-S(2)-C(20)	101.1 (8)	Zn(1)-N(1)-C(5)	125.8 (17)
Zn(1)-S(3)-C(9)	95.6 (6)	S(1)-C(10)-C(11)	112.2 (14)
Zn(1)-S(3)-C(30)	92.9 (6)	S(2)-C(20)-C(21)	116.6 (9)
C(9)-S(3)-C(30)	106.8 (9)	S(3)-C(30)-C(31)	106.7 (13)
Zn(1)-S(4)-C(40)	104.4 (8)	S(4)-C(40)-C(41)	115.2 (11)
Zn(1)-N(1)-C(1)	123.5 (9)	S(3)-C(30)-C(40)	121.3 (15)
S(1)-C(10)-C(20)	125.4 (17)	S(4)-C(40)-C(30)	124.8 (16)
S(2)-C(20)-C(10)	118.6 (11)		

not exceed $0.85 \text{ e} \text{ \AA}^{-3}$. The systematic absences observed in the data sets of 2 and 5 allowed the unambiguous assignment of the space groups given in Table I. In the case of 3, there were no systematic absences, which indicated a choice between the space groups $P1$ and $P\bar{1}$ in the triclinic crystal system. The measured density (floatation method) suggested $Z = 1$. Space group $P\bar{1}$ would require a center of inversion on the molecule and was therefore rejected in favor of $P1$. Even in $P1$, it was observed that only the sulfur ligand has a well-defined position. There appear to be two positions for the dmapy ligand, but these are not clearly evident and the ligand therefore appears as severely distorted with unusual C-C and N-C distances; for Zn, two disordered positions at a distance of 1.364 (3) Å are evident. Figure 3 shows the least distorted structure. In view of this situation, possible transformations of the lattice to a higher symmetry space group were investigated. In all the cases the discrepancies in the transformed lattice dimensions were well beyond experimental error, and there were clear differences in the intensities of supposedly equivalent reflections. Accordingly, the space group assignment $P1$ was maintained. No evidence for secondary extinction was found.

Positional and thermal parameters, interatomic distances and bond angles, and cell-packing diagrams are given as supplementary material. Selected interatomic distances and bond angles are given in Tables II-IV, and perspective drawings of the structures are given in Figures 1-3.

Results

While complex 2 and its adducts 3 and 4 with dmapy and py are colorless as expected, the bpy adduct 5 is orange in the solid

Table IV. Selected Geometrical Data for 5

Distances (Å)			
Zn-S(3)	2.275 (3)	Zn-S(1)	2.292 (3)
Zn-S(2)	3.214 (3)	Zn-N(2)	2.104 (8)
Zn-N(1)	2.090 (7)	S(2)-C(2)	1.774 (10)
S(1)-C(1)	1.782 (10)	S(3)-C(3)	1.790 (9)
S(2)-C(5)	1.806 (13)	S(4)-C(6)	1.800 (10)
S(4)-C(4)	1.794 (10)		

Angles (deg)			
S(1)-Zn-S(3)	112.6 (1)	S(1)-Zn-N(1)	132.3 (2)
S(3)-Zn-N(1)	108.0 (2)	S(1)-Zn-N(2)	100.4 (2)
S(3)-Zn-N(2)	121.4 (2)	N(1)-Zn-N(2)	78.0 (3)
S(1)-Zn-S(2)	65.2 (1)	S(2)-Zn-S(3)	98.2 (3)
S(2)-Zn-N(1)	85.5 (3)	S(2)-Zn-N(2)	140.1 (2)
Zn-S(1)-C(1)	98.6 (3)	C(2)-S(2)-C(5)	103.7 (6)
Zn-S(3)-C(3)	103.0 (3)	C(4)-S(4)-C(6)	104.6 (5)
Zn-N(1)-C(51)	125.7 (7)	Zn-N(1)-C(55)	115.4 (6)
C(51)-N(1)-C(55)	118.8 (8)	Zn-N(2)-C(56)	116.1 (6)
Zn-N(2)-C(60)	125.1 (7)	C(56)-N(2)-C(60)	118.8 (8)
S(1)-C(1)-C(2)	120.8 (8)	S(1)-C(1)-C(11)	116.6 (6)
C(2)-C(1)-C(11)	122.6 (8)	S(2)-C(2)-C(1)	117.1 (8)
S(2)-C(2)-C(21)	118.1 (6)	C(1)-C(2)-C(21)	124.7 (8)
S(3)-C(3)-C(4)	120.2 (8)	S(3)-C(3)-C(31)	115.7 (6)
C(4)-C(3)-C(31)	124.1 (8)	S(4)-C(4)-C(3)	117.5 (7)
S(4)-C(4)-C(41)	117.6 (6)	C(3)-C(4)-C(41)	124.9 (9)

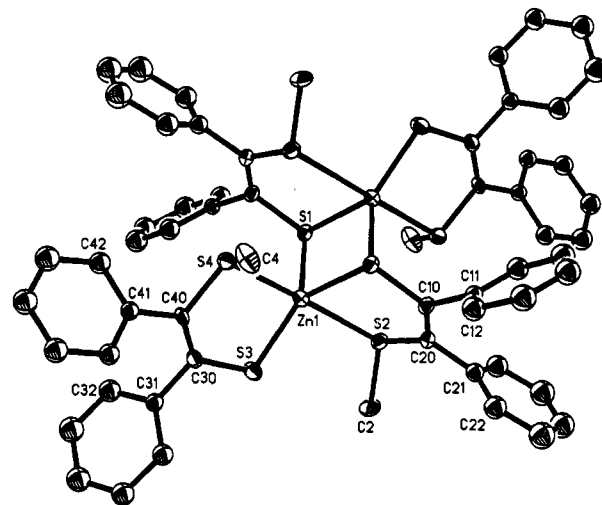


Figure 1. Perspective view of 2 with 30% probability ellipsoids.

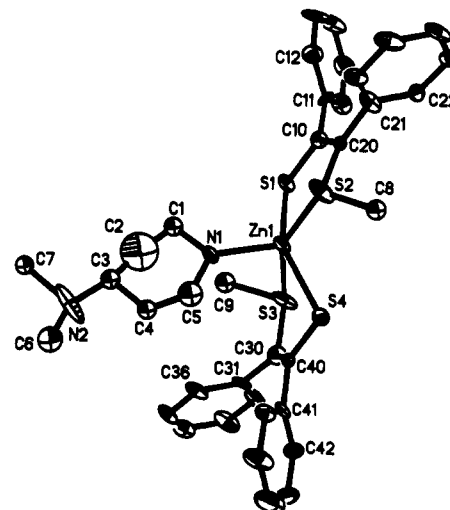


Figure 2. Perspective view of 3 with 30% probability ellipsoids.

state and in solution, which is unusual for a zinc complex. The color originates from an absorption with an ϵ_{max} at 450 nm which is assigned to an $n(\text{=S:}) \rightarrow \pi^*(\text{bpy})$ transition. On thermolysis, 2 decomposes with disproportionation of the sulfur ligands, as was

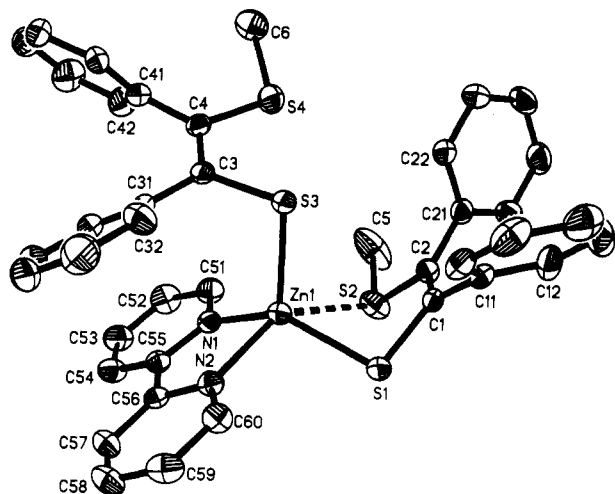


Figure 3. Perspective view of **5** with 30% probability ellipsoids.

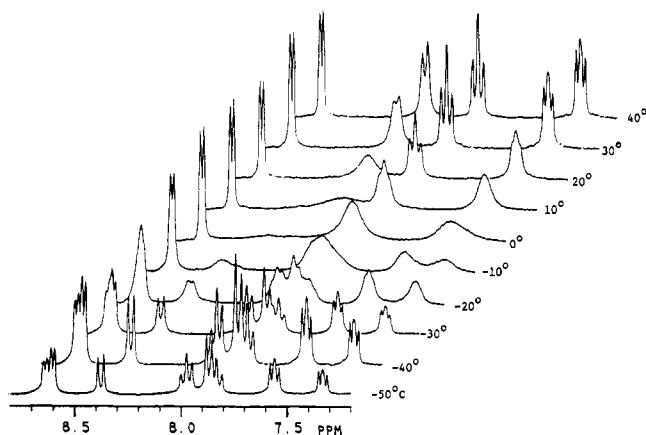
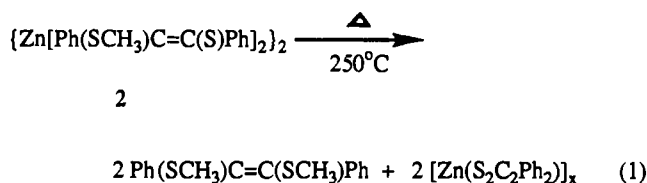


Figure 4. Variable-temperature ^1H NMR signals of the bipyridyl protons for the mixture of free bipyridine and **5** in CDCl_3 at different temperatures.

previously observed with the corresponding nickel complex⁶ (eq 1); the thermolysis of the nitrogen base adducts proceeds similarly



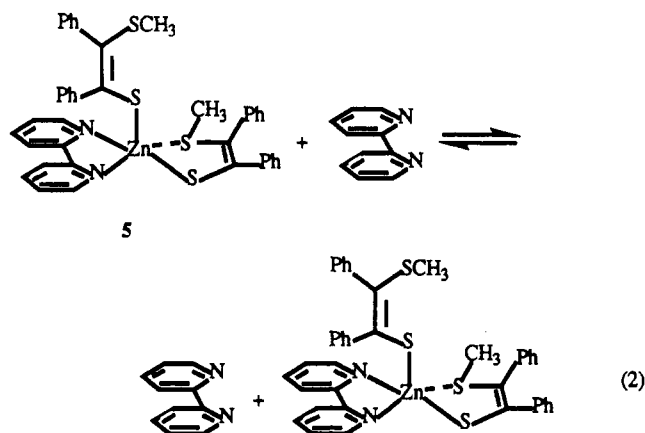
with prior loss of the nitrogen bases dmapy, py, and bpy, respectively.

Variable-temperature ^1H NMR measurements of **2** in dry CDCl_3 produced no evidence for dynamic behavior similar to that previously observed in the corresponding Ni(II) complex,⁶ suggesting that sulfur–ligand inversion or structural isomerization reactions in **2** are prevented presumably due to steric hindrance introduced by the formation of μ -S bridge bonds.

^1H NMR measurements of **2** in moist CDCl_3 provided evidence for the presence of equilibrium amounts of a hydrate adduct, which, however, was too unstable to be isolated. While the more stable and isolable py and dmapy adducts **3** and **4** also showed no dynamic behavior on the NMR time scale, exchange reactions involving the nitrogen bases evidently are taking place, which appear to be fast at -80°C , as even at this low temperature only broad signals of the protons of the free and bound nitrogen bases are observed.

Although **5** contains nonequivalent sulfur ligands in the solid state, as evidenced by X-ray crystallographic analysis to be described below, they are equivalent in solution, since the ^1H NMR spectra of **5** in CDCl_3 show only one signal of the S– CH_3 protons.

Furthermore, analysis of mixtures of **5** with free bpy by variable-temperature ^1H NMR spectroscopy reveals the coordinated bpy to be exchangeable with free bpy (see Figure 4). This exchange could be facilitated by the sulfur ligands ($-\text{SCH}_3$ on-off equilibria). See eq 2. The coordinated bpy in **5** was also found to readily exchange with free dmapy in solution.



The structure of **2** in the solid state as determined by a single-crystal X-ray analysis reveals a dimeric S-bridged structure with two equivalent pentacoordinated Zn atoms in a trigonal-bipyramidal environment. Table II shows that the axial Zn–S bond lengths are 2.712 (3) and 2.548 (3) Å, while the equatorial Zn– μ -S bonds are 2.383 (3) and 2.450 (3) Å, respectively, indicating a slight asymmetry of the Zn–S–Zn bonds. The two remaining equatorial Zn–S bonds of 2.270 (3) Å are shorter than the axial Zn–S bonds, all are within normal ranges.⁷ The S–Zn–S bond angles also show deviations from ideal trigonal-bipyramidal symmetry, attributable to the presence of the Zn_2S_2 moiety and crystal packing effects.

The dmapy adduct **3** is monomeric and contains a pentacoordinated Zn atom in a distorted square-pyramidal ligand environment. While the sulfur ligand positions in the lattice are well-defined, there is considerable disorder involving the dmapy ligand and the Zn ion, both occupying two disordered positions, only one set of which is shown in Figure 2. The mean Zn–S (thiolato) and Zn–S (thioether) bond lengths are 2.513 (7) and 2.831 (7) Å, respectively. The Zn–N distance is only 2.069 (10) Å, indicating a strong bonding interaction.

In the bpy adduct **5**, whose structure is shown in Figure 3, the bpy ligand is bound symmetrically to zinc with mean Zn–N bond lengths of 2.097 (8) Å, and the N–Zn–N bond angle is 78.0° . The two Zn–S (thiolato) bonds are almost equal, their average length of 2.283 (8) Å being shorter than the corresponding bonds in **2**. One sulfur ligand is bidentate, but the coordinative Zn–S(CH_3) bond has the length of 3.214 (3) Å and is evidently weak; it is still shorter than the sum of the van der Waals radii of zinc and sulfur (3.25 Å), however. The other sulfur ligand is monodentate and shows the S(CH_3) group in a completely noninteracting position. The zinc atom in **5** thus is pentacoordinated. To differentiate the coordination geometries of zinc from distorted tetrahedral and distorted square pyramidal, the mean plane passing through S₁, S₂, N₁, N₂ was calculated. The S atoms are alternately above and below this plane by 0.02 Å; Zn is present at a distance of 0.84 Å from this plane. The average value of the angles S(3)–Zn–S(1), S(3)–Zn–S(2), S(3)–Zn–N(1), and S(3)–Zn–N(2) is $110(4)^\circ$, and it is thus concluded that the geometry about zinc is distorted square pyramidal rather than distorted tetrahedral.

Discussion

This study indicates that zinc has a clear preference for pentacoordination in neutral complexes with S and S,N ligand cores even under conditions where tetra- and hexacoordinated structures

(7) (a) Dance, I. *Polyhedron* **1986**, 1037. (b) Blower, P. J.; Dilworth, J. R. *Coord. Chem. Rev.* **1987**, 76, 121.

could be realized with equal probability. This result is of interest, as two previously proposed⁸ structural models of the zinc binding sites in DNA-binding proteins,⁹ Zn(S-2,4,6-iPr₃C₆H₂)₂(bpy) (**7**) and Zn(S-2,3,5,6-Me₄C₆H₂)₂(Me-imid)₂ (**8**), where iPr = *i*-C₃H₇ and Me-imid = *N*-methylimidazole, both contain tetracoordinate Zn(II) in distorted-tetrahedral ligand environments and neither exhibits a tendency to form pentacoordinated adducts with nitrogen bases. The failure of **7** and **8** to form pentacoordinated adducts may be due to the high electron densities on zinc caused by the strong bonding interactions with the powerfully nucleophilic substituted thiophenolato ligands. It should be noted that neither **7** nor **8** formed an adduct with CH₃CN, under the same conditions where a closely related Co(II) complex produced the pentacoordinated 1:1 adduct Co(S-2,6-iPr₂C₆H₃)₂(bpy)(CH₃CN) (**9**).¹⁰ Evidently, Co(II) may accommodate another donor ligand because the high electron density on cobalt is offset by the availability of d orbitals for back-bonding. However, with appropriate ligands, even Zn(II) reveals its tendency to form pentacoordinated structures and actually favors pentacoordination over tetracoordination.

This study also indicates that **5** is the maximally attainable coordination number in neutral zinc complexes with sulfur and nitrogen ligands. We believe that this result can be generalized and that it has biological significance inasmuch as it suggests the plausibility of pentacoordinated zinc especially in the functional states zinc proteins and enzymes. Which coordination number is ultimately realized appears to depend primarily on the effective

electron density on zinc. While tricoordinated structures may be confirmed to anionic complexes such as exemplified by the recently characterized⁴ anion Zn(SR)₃⁻, in neutral complexes pentacoordination is favored over tetracoordination only at low electron densities on zinc. Depending on the donor strengths of the ligands, limiting cases may result in which pentacoordination is only barely favored over tetracoordination. Such is the case in **5**, where the bpy ligand still permits one of the two sulfur ligands to remain bidentate, although the coordinate Zn–S(CH₃) bond is quite weak. The other sulfur ligand in **5** is forced to adopt a monodentate coordination in which the S–CH₃ group is in a clearly noninteractive position in the solid state. This arrangement is not necessarily retained in solution, as the free S(CH₃) group could interact dynamically with zinc in solution. This interaction may facilitate the exchange of coordinated bpy with free bpy, as suggested by the variable-temperature ¹H NMR measurements; since Co(II) and other metals may substitute Zn(II) in DNA-binding proteins and enzymes and this heterometallic substitution has been suggested¹¹ as relevant to the mechanisms of metal toxicity, teratogenicity, or carcinogenicity, similar studies will now be conducted on thiol–thioether complexes of other elements.

Acknowledgment. Support of the research by the National Science Foundation is gratefully acknowledged.

Supplementary Material Available: For complexes **2**, **3**, and **5**, tables of atomic positions, scattering factors, least-squares planes, thermal parameters, bond distances, and bond angles, crystal lattice diagrams, tables and test describing crystallographic details, and a textual presentation of VT NMR data for Figure 4 (42 pages); listings of observed and calculated structure factors (64 pages). Ordering information is given on any current masthead page.

- (8) Corwin, D. T.; Koch, S. A. *Inorg. Chem.* **1988**, *27*, 493.
 (9) (a) Diakun, G. P.; Fairall, L.; Klug, A. *Nature (London)* **1986**, *324*, 698.
 (b) Wu, F. Y.-H.; Wu, C.-W. *Annu. Rev. Nutr.* **1987**, *7*, 251 and references cited therein.
 (10) Koch, S. A.; Fikar, R.; Millar, M.; O'Sullivan, T. *Inorg. Chem.* **1984**, *23*, 122.

- (11) Sunderman, F. W., Jr.; Barber, A. M. *Ann. Clin. Lab. Sci.* **1988**, *18*, 267.

Contribution from the Laboratoire de Chimie Organo-Minérale, UA 422 au CNRS, Faculté de Chimie, 1 Rue Blaise Pascal, F-67000 Strasbourg, France

A Bis(terpyridine)ruthenium(II) Catenate

Jean-Pierre Sauvage* and Michael Ward

Received March 13, 1991

A new catenate has been synthesized that contains a pseudooctahedral coordination site and a ruthenium(II) center. The compound is built by entwining two functionalized terpyridine derivatives around the metal prior to cyclizing the system. The yield for the double cyclization step (four phenolate groups of the precursor complex and 2 equiv of the diiodo derivative of hexaethylene glycol) is modest (11%) but allows preparation of several tens of milligrams per experiment. The catenate obtained consists of two interlocked 38-membered rings. The ruthenium(II) catenate is nonluminescent at room temperature in CH₃CN, similar to other bis(terpyridine) complexes. Demetalation of the free catenand has not yet been carried out.

Introduction

In the last few years we have been interested in the synthesis and study of coordinating molecular systems consisting of two or more interlocked rings.¹ Catenanes in general have been discussed in relatively old literature, and various synthetic approaches have been suggested and developed.^{2,3}

An efficient synthesis of interlocked rings has recently been developed. It is based on a three-dimensional template synthesis around a transition-metal ion.^{4–8} Cu(I) is used to bind two

molecules of a 2,9-disubstituted 1,10-phenanthroline: in the tetrahedral complex the two ligands are mutually perpendicular and organized into an arrangement such that cyclization of each phenanthroline fragment leads to two interlocked rings (Scheme 1). The resulting copper complex (a *catenate*) is readily demetalated with cyanide to give the free ligand (a *catenand*).

These ligands have a variety of interesting properties. The geometry of the ligand changes considerably between the free and bound forms,⁹ an air-stable nickel(I) complex has been prepared,¹⁰

- (1) Chambron, J.-C.; Dietrich-Buchecker, C. O.; Hemmert, C.; Khemiss, A. K.; Mitchell, D.; Sauvage, J.-P.; Weiss, J. *Pure Appl. Chem.* **1990**, *62*, (6), 1027 (and references therein).
 (2) Schill, G. *Catenanes, Rotaxanes and Knots*; Academic Press: New York, 1971 (and references therein).
 (3) Wasserman, E. *J. Am. Chem. Soc.* **1960**, *82*, 4433.
 (4) Dietrich-Buchecker, C. O.; Sauvage, J.-P.; Kintzinger, J.-P. *Tetrahedron Lett.* **1983**, *24*, 5095.

- (5) Dietrich-Buchecker, C. O.; Sauvage, J.-P.; Kern, J.-M. *J. Am. Chem. Soc.* **1984**, *106*, 3043.
 (6) Sauvage, J.-P. *Nouv. J. Chim.* **1985**, *9*, 299.
 (7) Dietrich-Buchecker, C. O.; Sauvage, J.-P. *Chem. Rev.* **1987**, *87*, 795.
 (8) Dietrich-Buchecker, C. O.; Sauvage, J.-P. *Tetrahedron* **1990**, *46* (2), 503.
 (9) Cesario, M.; Dietrich-Buchecker, C. O.; Guilhem, J.; Pascard, C.; Sauvage, J.-P. *J. Chem. Soc., Chem. Commun.* **1985**, 244.